

# Preparation, Characterization, and Time-Resolved Fluorometric Application of Silica-Coated Terbium(III) Fluorescent Nanoparticles

Zhiqiang Ye, Mingqian Tan, Guilan Wang, and Jingli Yuan\*

Department of Analytical Chemistry, Dalian Institute of Chemical Physics, Chinese Academy of Sciences, Dalian 116012, P. R. China

**Novel silica-coated terbium(III) chelate fluorescent nanoparticles have been prepared and characterized as a new type of fluorescence probe for highly sensitive time-resolved fluorescence bioassay. The preparation was carried out in a water-in-oil microemulsion containing a strongly fluorescent Tb<sup>3+</sup> chelate, *N,N,N',N'*-[2,6-bis(3'-aminomethyl-1'-pyrazolyl)-phenylpyridine]tetrakis(acetate)-Tb<sup>3+</sup>, Triton X-100, hexanol, and cyclohexane by controlling hydrolysis of tetraethyl orthosilicate. The nanoparticles are spherical and uniform in size, 42 ± 3 nm in diameter, strongly fluorescent, and highly photostable and have enough of a long fluorescence lifetime (1.52 ms) for time-resolved fluorescence measurement. A stable and non-toxic method was developed for the surface modification and protein immobilization of the nanoparticles. As a model of application, the nanoparticle-labeled streptavidin was prepared and used in a sandwich-type time-resolved fluoroimmunoassay of human prostate-specific antigen (PSA) by using a 96-well microtiter plate as the solid-phase carrier. The method gives a detection limit of 7.0 pg/mL for the PSA assay.**

Ultrasensitive nonisotopic bioassays have been rapidly developed for clinical diagnostics and biological research in recent years. In these areas, fluorescent lanthanide chelates are very noticeable as fluorescence probes for highly sensitive time-resolved fluoroimmunoassay (TR-FIA), DNA hybridization assay, and fluorescence imaging microscopy due to the effective elimination of background fluorescence.<sup>1–4</sup> However, the fluorescence of lanthanide chelates is weaker compared with the organic fluorescence dyes since the fluorescence quantum yields and molar extinction coefficients of the chelates are generally smaller than those of the organic fluorescence dyes. Photobleaching is still inevitable when a lanthanide chelate label is excited with continuous exposure under an intense excitation source for monitoring some real-time biological processes and sensitive detection, such as fluorescence bioimaging,<sup>5</sup> even though the

fluorescence of the chelate is more photostable than that of the organic dye. Furthermore, it is known that only a few lanthanide chelates are suitable to be used as fluorescence probes for bioassays, which also prevents the effective application of time-resolved fluorometry.

Recently, nanometer-sized luminescent materials have become a research attraction for their applications as luminescence probes in various types of biological detection. The representative luminescent nanoparticle probes include semiconductor nanoparticles (quantum dots),<sup>6–9</sup> plasmon-resonant nanoparticles,<sup>10</sup> gold nanoparticles,<sup>11</sup> and dye-doped silica nanoparticles.<sup>12,13</sup> Compared with conventional organic dyes, the luminescent nanoparticles have higher photostability and stronger luminescence, which allows them favorably to be used as luminescence probes for bioassays. The main problem using the nanoparticle luminescence probes in bioassays is that the luminescence measurement is easily affected by the strong nonspecific scattering lights, such as Tyndall, Rayleigh, and Raman scatterings.

Polystyrene latex nanoparticles containing a high concentration of a Eu<sup>3+</sup> fluorescent chelate have also been developed as the probe for highly sensitive TR-FIA.<sup>14–17</sup> Because a latex nanoparticle probe can contain too many Eu<sup>3+</sup> fluorescence chelate molecules (30 000 Eu<sup>3+</sup> fluorescent chelate molecules/107-nm particle),<sup>15</sup> the sensitivity of TR-FIA using the europium latex nanoparticle probe is very high.<sup>17</sup> However, the polystyrene latex nanoparticle probe has the drawbacks of large size (>100 nm), easy agglomeration

\* To whom correspondence should be addressed. Tel: +86-411-3693509. Fax: +86-411-3693509. E-mail: jingliyuan@yahoo.com.cn.

- (1) Soini, E.; Lövgren, T. *CRC Crit. Rev. Anal. Chem.* **1987**, *18*, 105–154.
- (2) Diamandis, E. P.; Christopoulos, T. K. *Anal. Chem.* **1990**, *62*, 1149A–1957A.
- (3) Dickson, E. F. G.; Pollak, A.; Diamandis, E. P. *Pharmacol. Ther.* **1995**, *66*, 207–235.
- (4) Hemmälä, I.; Mukkala, V.-M. *Crit. Rev. Clin. Lab. Sci.* **2001**, *38*, 441–519.

- (5) Seveus, L.; Väisälä, M.; Syrjänen, S.; Sandberg, M.; Kuusisto, A.; Harju, R.; Salo, J.; Hemmälä, I.; Kojola, H.; Soini, E. *Cytometry* **1992**, *13*, 329–338.
- (6) Bruchez, M. Jr.; Moronne, M.; Gin, P.; Weiss, S.; Alivisatos, A. P. *Science* **1998**, *281*, 2013–2016.
- (7) Chan, W. C. W.; Nie, S. *Science* **1998**, *281*, 2016–2018.
- (8) Taylor, J. R.; Fang, M. M.; Nie, S. *Anal. Chem.* **2000**, *72*, 1979–1986.
- (9) Mitchell, G. P.; Mirkin, C. A.; Letsinger, R. L. *J. Am. Chem. Soc.* **1999**, *121*, 8122–8123.
- (10) Schultz, S.; Smith, D. R.; Mock, J. J.; Schultz, D. A. *Proc. Natl. Acad. Sci. U.S.A.* **2000**, *97*, 996–1001.
- (11) Hayat, M. A. *Colloidal Gold: Principles, Methods and Applications*; Academic Press: New York, 1989.
- (12) Santra, S.; Zhang, P.; Wang, K.; Tapeç, R.; Tan, W. *Anal. Chem.* **2001**, *73*, 4988–4993.
- (13) Santra, S.; Wang, K.; Tapeç, R.; Tan, W. *J. Biomed. Opt.* **2001**, *6*, 160–166.
- (14) Härmä, H.; Soukka, T.; Lönnberg, S.; Paukkunen, J.; Tarkkinen, P.; Lövgren, T. *Luminescence* **2000**, *15*, 351–355.
- (15) Härmä, H.; Soukka, T.; Lövgren, T. *Clin. Chem.* **2001**, *47*, 561–568.
- (16) Soukka, T.; Härmä, H.; Paukkunen, J.; Lövgren, T. *Anal. Chem.* **2001**, *73*, 2254–2260.
- (17) Soukka, T.; Paukkunen, J.; Härmä, H.; Lönnberg, S.; Lindroos, H.; Lövgren, T. *Clin. Chem.* **2001**, *47*, 1269–1278.

in aqueous medium due to their hydrophobic property, and difficulty in separating from solution in the surface modification and labeling processes. Several kinds of silica-coated material (or compound) nanoparticles have been prepared including Ag/SiO<sub>2</sub>,<sup>18,19</sup> Au/SiO<sub>2</sub>,<sup>20</sup> magnetic material/SiO<sub>2</sub>,<sup>21–24</sup> CdS/SiO<sub>2</sub>,<sup>25,26</sup> and 2,2'-bipyridine–Ru<sup>2+</sup> chelate/SiO<sub>2</sub><sup>12</sup> nanoparticles. Compared with the latex fluorescent nanoparticle probe, the silica fluorescent nanoparticle probe is highly hydrophilic and easy to centrifuge for separation in preparation, surface modification, and labeling procedures.<sup>12</sup>

In the present work, the silica-coated *N,N,N',N'*-[2,6-bis(3'-aminomethyl-1'-pyrazolyl)-phenylpyridine]tetrakis(acetate)–Tb<sup>3+</sup> (BPTA–Tb<sup>3+</sup>) chelate<sup>27</sup> fluorescent nanoparticles were prepared, characterized, and developed as a uniform, stable, and sensitive fluorescence probe for time-resolved fluorescence bioassay. As a new analytical reagent, the novel nanoparticle fluorescence probe combined the advantages of both luminophore-doped silica nanoparticle probe and lanthanide latex fluorescence probe including smaller size (<50 nm), high hydrophilicity, and biocompatibility, easy to modify to attach biomolecules, and easy to eliminate the nonspecific scattering lights by using time-resolved fluorescence measurement since the fluorescence of the nanoparticle probe is long-lived. Furthermore, the photostability against photobleaching of the Tb<sup>3+</sup> chelate in nanoparticles was remarkably increased compared with the free Tb<sup>3+</sup> chelate due to the outside silica protection. A stable and nontoxic method was developed for the surface modification and protein immobilization of the nanoparticles. The nanoparticle-labeled streptavidin (SA), which can be used for solid-phase time-resolved fluorescence bioassays, was prepared. Because the nanoparticles containing a high concentration of the Tb<sup>3+</sup> chelate are strongly fluorescent, the sensitivity of the time-resolved fluorescence bioassay has been remarkably improved by using the nanoparticles as fluorescence probe. The TR-FIA of human prostate-specific antigen (PSA) using the nanoparticle-labeled SA shows that the method is highly sensitive with good precision.

## EXPERIMENTAL SECTION

**Materials and Physical Measurements.** The BPTA–Tb<sup>3+</sup> chelate was synthesized by using a previous method.<sup>27</sup> (3-Aminopropyl)triethoxysilane, tetraethyl orthosilicate (TEOS), and Triton X-100 were purchased from Acros Organics. SA was purchased from Chemicon International Inc. Mouse monoclonal and goat polyclonal anti-human PSA antibodies were purchased

from OEM Concepts Co. Sulfosuccinimidyl-6-(biotinamido)hexanoate (NHS-LC-biotin) was purchased from Pierce Chemical Co. The standard solutions of human PSA were prepared by diluting human PSA antigen (Biogenesis Ltd.) with 0.05 M Tris-HCl buffer, pH 7.8, containing 5% bovine serum albumin (BSA), 0.9% NaCl, and 0.1% NaN<sub>3</sub>. A JEOL model JEM-2000EX transmission electron microscope was used for measuring the shape and size of the nanoparticles. Fluorescence spectra and emission lifetimes were measured on the Perkin-Elmer LS 50B spectrofluorometer. The TR-FIA was carried out with a FluoroNunc 96-well microtiter plate as solid-phase carrier and measured on the Perkin-Elmer Victor 1420 multilabel counter with the conditions of excitation wavelength, 320 nm, emission wavelength, 545 nm, delay time, 0.2 ms, and window time, 0.4 ms.

**Preparation of the Nanoparticles.** A water-in-oil (W/O) microemulsion containing 2.38 g of Triton X-100, 1.88 g of hexanol, 7.25 g of cyclohexane, 200  $\mu$ L of TEOS, and 1.1 mL of an aqueous solution of 160 mg of BPTA–Tb<sup>3+</sup> was mixed with a W/O microemulsion containing 2.38 g of Triton X-100, 1.88 g of hexanol, 7.25 g of cyclohexane, and 200  $\mu$ L of concentrated ammonium hydroxide with vigorous stirring. After stirring for 24 h, the precipitation was obtained by adding acetone, centrifuging, and washing with ethanol and water several times to remove surfactant and unreacted materials. The obtained white silica-coated Tb<sup>3+</sup> chelate fluorescent nanoparticles were dried in desiccator for the following use.

**Surface Modification of the Nanoparticles.** A mixture of 10 mg of nanoparticles and 2 g of (3-aminopropyl)triethoxysilane was refluxed in 20 mL of toluene for 24 h under N<sub>2</sub>. After centrifuging, the nanoparticles were washed with ethanol and water. The nanoparticles were suspended in 4.5 mL of 0.1 M sodium acetate buffer, pH 4.9, and a mixture of 2,4,6-trichloro-1,3,5-triazine (0.6 mg), acetone (3.0 mL), and H<sub>2</sub>O (3.0 mL) was added. After stirring for 1 h at room temperature, the nanoparticles were centrifuged and washed with acetone and water. The nanoparticles were added to a solution of 20 mg of BSA in 1.0 mL of 0.1 M NaHCO<sub>3</sub>, pH 8.5. After being stirred at 4 °C for 24 h, the nanoparticles were centrifuged and washed with water. The surface-modified nanoparticles were stored at 4 °C for the following use.

**Preparation of the Nanoparticle-Labeled SA.** The surface-modified nanoparticles were suspended in 1.0 mL of 0.1 M phosphate buffer, pH 7.0, and 1.0 mg of SA and 0.1 mL of 1% glutaraldehyde were added. After stirring at 4 °C for 24 h, 2 mg of NaBH<sub>4</sub> was added, and the suspension was incubated at room temperature for 2 h. After being centrifuged and washed with phosphate buffer and water, the nanoparticle-labeled SA was further purified by gel filtration chromatography with the following conditions: mobile phase, 0.05 M NH<sub>4</sub>HCO<sub>3</sub>, 1.0  $\times$  29.1 cm Sephadex G-50 column, and flow rate of 1.0 mL/90 s. The fractions containing the nanoparticle-labeled SA were collected, diluted with 0.05 M Tris-HCl buffer, pH 7.8, containing 0.2% BSA, 0.1% NaN<sub>3</sub>, and 0.9% NaCl, and stored at 4 °C before use.

**Preparation of Biotinylated Goat Anti-Human PSA Antibody.** After two dialyses of 1.0 mL of goat anti-human PSA antibody solution (0.5 mg/mL) for 24 h at 4 °C against 3 L of saline water, 8.4 mg of NaHCO<sub>3</sub> and 3 mg of NHS-LC-biotin were added with stirring. After stirring for 1 h at room temperature,

- (18) Ung, T.; Liz-Marzán, L. M.; Mulvaney, P. *Langmuir* **1998**, *14*, 3740–3748.
- (19) Li, T.; Moon, J.; Morrone, A. A.; Mecholsky, J. J.; Talham, D. R.; Adair, J. H. *Langmuir* **1999**, *15*, 4328–4334.
- (20) Liz-Marzán, L. M.; Giersig, M.; Mulvaney, P. *Langmuir* **1996**, *12*, 4329–4335.
- (21) López Pérez, J. A.; López Quintela, M. A.; Mira, J.; Rivas, J.; Charles, S. W. *J. Phys. Chem. B* **1997**, *101*, 8045–8047.
- (22) Dresco, P. A.; Zaitsev, V. S.; Gambino, R. J.; Chu, B. *Langmuir* **1999**, *15*, 1945–1951.
- (23) Liu, C.; Zou, B.; Rondinone, A. J.; Zhang, Z. J. *J. Phys. Chem. B* **2000**, *104*, 1141–1145.
- (24) Santra, S.; Tapeç, R.; Theodoropoulou, N.; Dobson, J.; Hebard, A.; Tan, W. *Langmuir* **2001**, *17*, 2900–2906.
- (25) Correa-Duarte, M. A.; Giersig, M.; Liz-Marzán, L. M. *Chem. Phys. Lett.* **1998**, *286*, 497–501.
- (26) Farmer, S. C.; Patten, T. E. *Chem. Mater.* **2001**, *13*, 3920–3926.
- (27) Yuan, J.; Wang, G.; Majima, K.; Matsumoto, K. *Anal. Chem.* **2001**, *73*, 1869–1876.

the solution was further incubated for 24 h at 4 °C. The solution was twice dialyzed each for 24 h at 4 °C against 3 L of 0.1 M NaHCO<sub>3</sub> containing 0.25 g of NaN<sub>3</sub>, and then 5 mg of BSA and 5 mg of NaN<sub>3</sub> were added. The solution was stored at -20 °C before use. When the biotinylated antibody solution was used for the immunoassay, it was diluted 300-fold with 0.05 M Tris-HCl buffer, pH 7.8, containing 0.2% BSA, 0.9% NaCl, and 0.1% NaN<sub>3</sub>.

**Immunoassay of Human PSA Using the Nanoparticle-Labeled SA.** After anti-human PSA monoclonal antibody (diluted to 10 µg/mL with 0.1 M carbonate buffer, pH 9.6) was coated on the wells (50 µL/well) of a 96-well microtiter plate by physical adsorption,<sup>28</sup> 45 µL of human PSA standard solution was added to each well. The plate was incubated at 37 °C for 1 h and washed with 0.05 M Tris-HCl buffer, pH 7.8, containing 0.05% Tween 20 and 0.05 M Tris-HCl buffer, pH 7.8. Then the biotinylated antibody (~1.1 µg/mL, 45 µL/well) was added to each well, and the plate was incubated at 37 °C for 1 h. After washing, the nanoparticle-labeled SA (~1.0 µg/mL, 45 µL/well) was added to each well, and the plate was incubated at 37 °C for 1 h. The plate was washed four times with 0.05 M Tris-HCl buffer, pH 7.8, containing 0.05% Tween 20, and subjected to solid-phase time-resolved fluorometric measurement.

**Immunoassay of Human PSA Using the BPTA-Tb<sup>3+</sup>-Labeled SA.** The TR-FIA was carried out with the same method as described above by using the BPTA-Tb<sup>3+</sup> chelate-labeled SA<sup>27</sup> instead of the nanoparticle-labeled SA.

## RESULTS AND DISCUSSION

### Preparation and Characterization of the Nanoparticles.

The nanoparticles were prepared by hydrolysis of TEOS with ammonium hydroxide in a W/O microemulsion containing aqueous solution of BPTA-Tb<sup>3+</sup> chelate, surfactant Triton X-100, cosurfactant hexanol, and oil-phase cyclohexane. As described in the reports,<sup>19,24,29</sup> in the W/O microemulsion, the aqueous phase containing Tb<sup>3+</sup> chelate formed innumerable nanodroplets (water pools) by the action of the surfactant and cosurfactant. There each nanodroplet acted as a nanoreactor for the synthesis of nanoparticles, and the nanoparticles were formed undergoing the hydrolysis and polymerization reactions of TEOS. Since the size of the nanoparticles is dependent on the size of the water pools, the size of the nanoparticles can be controlled and tuned by changing the water-to-surfactant molar ratio (in general, the higher ratio, the larger particle size).<sup>24</sup>

The silica-coated BPTA-Tb<sup>3+</sup> fluorescent nanoparticles were characterized by transmission electron microscopy (TEM) and fluorescence spectroscopic methods. As shown in Figure 1, the fluorescent nanoparticles are spherical and uniform in size, 42 ± 3 nm in diameter. Because the Tb<sup>3+</sup> chelate was aggregated to the water pool in the microemulsion while the silica network is being formed, the Tb<sup>3+</sup> chelate molecules can be observed as dark dots embedded inside the silica network (the inset TEM image in Figure 1) compared with the pure silica nanoparticles prepared by the same method. The time-resolved fluorescence spectra of the nanoparticles and pure BPTA-Tb<sup>3+</sup> chelate were also measured in aqueous solution (Figure 2). Different from the silica-

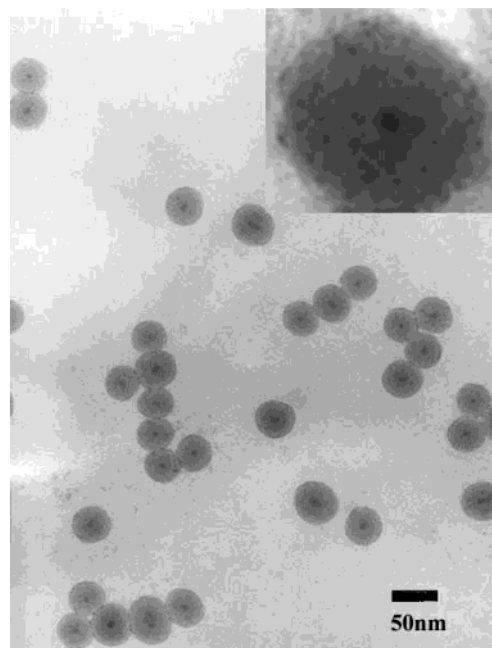


Figure 1. TEM image of silica-coated Tb<sup>3+</sup> chelate fluorescent nanoparticles at 100000× magnification (inset showing a higher resolution image of one nanoparticle at 200000× magnification).

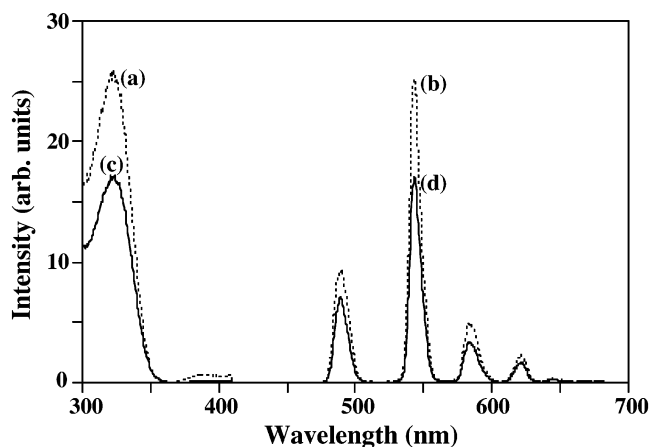


Figure 2. Time-resolved fluorescence excitation and emission spectra of pure BPTA-Tb<sup>3+</sup> chelate (0.1 µM, a, b) and the nanoparticles (2 mg/L, c, d) in water.

coated bipyridine-Ru<sup>2+</sup> chelate nanoparticles,<sup>12</sup> the excitation and emission spectra of the BPTA-Tb<sup>3+</sup> chelate nanoparticles and the pure BPTA-Tb<sup>3+</sup> chelate show the same spectrum patterns without any emission band shift. Assuming that the density of the nanoparticles is equal to pure silica (1.96 g/cm<sup>3</sup>),<sup>12</sup> the weight of one nanoparticle of 42 nm can be calculated ( $1.96 \times 4/3\pi r^3$ ) to be  $\sim 7.6 \times 10^{-17}$  g; thus, the concentration of the nanoparticle's solution used for Figure 2 (2 mg/L) corresponds to  $\sim 4.3 \times 10^{-11}$  M. According to the fluorescence intensities of Figure 2, the fluorescence of the nanoparticles is  $\sim 1500$ -fold stronger than that of the BPTA-Tb<sup>3+</sup> chelate at the same molar concentration. From this result, it also can be estimated that there are  $\sim 1500$  BPTA-Tb<sup>3+</sup> chelate molecules in a 42-nm nanoparticle if the silica network does not quench the fluorescence emission. However, the fluorescence lifetime of the Tb<sup>3+</sup> chelate nanoparticles in aqueous solution was measured to be 1.52 ms, which is shorter than that of the pure Tb<sup>3+</sup> chelate aqueous solution (2.68 ms).<sup>27</sup>

(28) Matsumoto, K.; Yuan, J.; Wang, G.; Kimura, H. *Anal. Biochem.* **1999**, *276*, 81–87.

(29) Arriagada, F. J.; Osseo-Asare, K. *J. Colloid Interface Sci.* **1999**, *211*, 210–220.



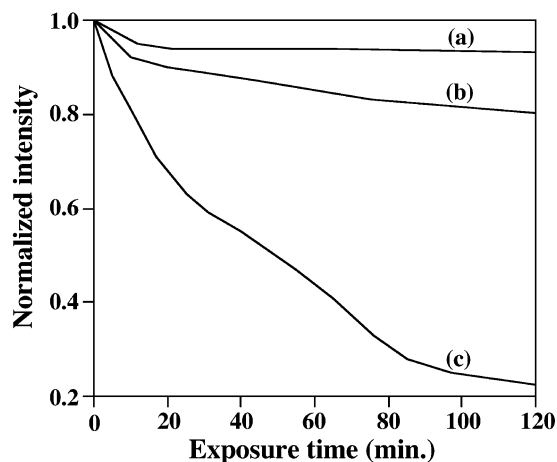


Figure 3. Photobleaching experiment: (a) the nanoparticles, (b) pure BPTA-Tb<sup>3+</sup> chelate, and (c) rhodamine B in aqueous solution phase with a 30-W deuterium lamp excitation source.

This fact indicates that the interaction between the silica network and the Tb<sup>3+</sup> ion existed in the nanoparticles even though the BPTA-Tb<sup>3+</sup> chelate is highly stable (higher than EDTA-Tb<sup>3+</sup>),<sup>30</sup> and this interaction is unfavorable for the fluorescence emission of the chelate.

**Photobleaching Experiments.** To evaluate the photostability of the nanoparticles, photobleaching experiments of the Tb<sup>3+</sup> chelate nanoparticles, pure BPTA-Tb<sup>3+</sup> chelate, and rhodamine B were performed in aqueous solution by using a 30-W deuterium lamp as an excitation source. The emission intensity was recorded at every 5-min interval for a period of 2 h. As shown in Figure 3, the emission intensities of rhodamine B and pure BPTA-Tb<sup>3+</sup> chelate solutions were decreased approximately 80 and 20%, respectively, in the period of 2 h, whereas the photobleaching of the nanoparticle's solution was slightly (less than 7%) in the same period. The high photostability of the nanoparticles is caused by the fact that the Tb<sup>3+</sup> chelate in the nanoparticles is coated by silica, which isolates the chelate from the outside environment, such as solvent molecules and free radicals caused by light exposure and, therefore, effectively protects the chelate from photodecomposition. Figure 3a also showed that photobleaching of the nanoparticles occurred mainly during the initial 0–20 min; this was explained by assuming that the Tb<sup>3+</sup> chelate molecules very close to the silica particle surface were photobleached during this period.

**Surface Modification of the Nanoparticles.** The surface of silica-coated Tb<sup>3+</sup> chelate fluorescent nanoparticles could be modified easily for binding biomolecules. As described in the literature report (Figure 4a),<sup>12</sup> surface modification by using the

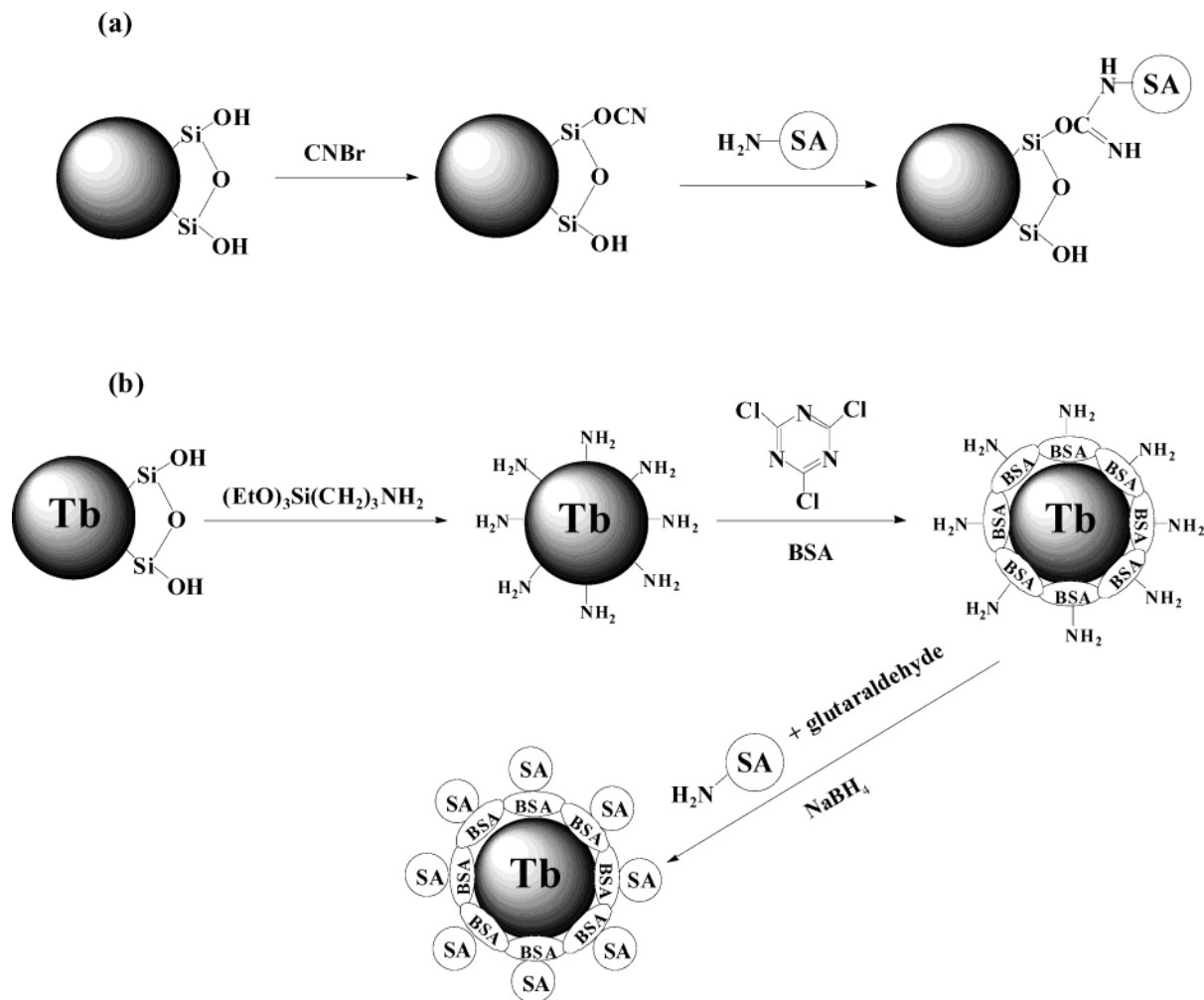


Figure 4. Schematic representation of surface modification and SA immobilization processes of the silica nanoparticles. (a) The nanoparticle's surface was modified by using the CNBr activation method, and then SA was immobilized onto the nanoparticle's surface. (b) The nanoparticle's surface was coated with BSA, and then SA was immobilized onto the nanoparticle's surface.

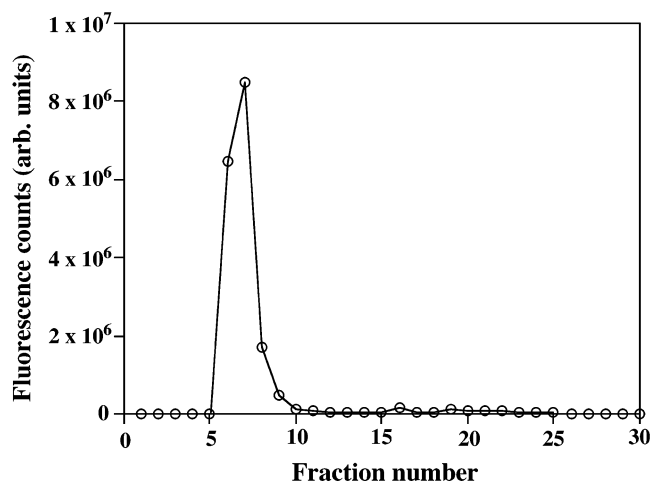


Figure 5. Separation of the silica-coated  $\text{Tb}^{3+}$  chelate fluorescent nanoparticle-labeled SA by gel filtration chromatography. Fractions collected were 1 mL each.

CNBr activation method is the most prevalent method on both laboratory and industrial scales because the procedure is relatively simple to carry out and is very reproducible. However, the CNBr surface activation technique has some severe disadvantages besides its toxicity. One of its main drawbacks is constant leakage of coupled ligand because of the instability of the isourea bond formed between the activated support and an amine-containing ligand. Moreover, isourea derivatives are positively charged at neutral pH, so the adsorbent is also a weak anion exchanger. The resulting ion-exchange properties of the affinity matrix may cause nonspecific binding.<sup>31</sup> For these reasons, a stable and nontoxic surface modification method was developed in the present work by using amino-coupling chemistries to overcome the deficiencies of the CNBr method.

After the nanoparticle's surface is silanized by (3-aminopropyl)-triethoxysilane,<sup>32</sup> the modified nanoparticles can be conjugated to protein directly. However, it was found that the nanoparticle-labeled SA (or antibody) prepared by this method could not be reacted to the biotinylated antibody (or antigen) on the solid-phase surface. This phenomenon might be due to the effect of strong steric hindrance between the rigid nanoparticle and the solid-phase surface since the labeled protein is tightly fixed on the surface of the nanoparticle in this case. As shown in Figure 4b, this problem was solved successfully by coating the amino-modified nanoparticles with BSA first, and then the BSA-coated nanoparticles were conjugated to SA. Because there is a flexible BSA "bridge" between the nanoparticle and SA in this case, the steric hindrance between the nanoparticle and solid-phase surface is decreased, and thus the labeled SA-biotinylated antibody reaction on the solid-phase surface can occur.

**Preparation of the Nanoparticle-Labeled SA.** The BSA-coated nanoparticles were conjugated to SA by coupling the amino groups of the modified nanoparticle and SA with glutaraldehyde.<sup>33</sup> In general, after centrifuging and washing, the nanoparticle-labeled

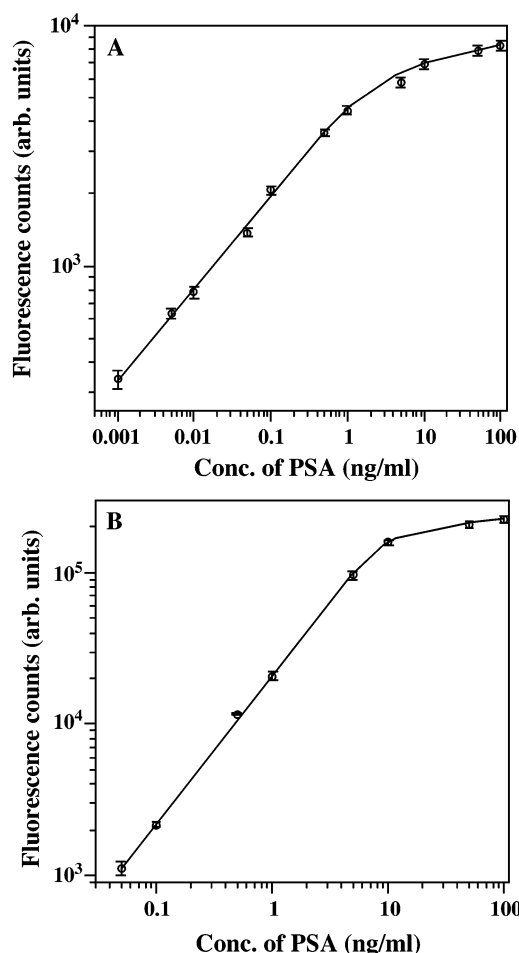


Figure 6. Calibration curves of TR-FIA by using the silica-coated  $\text{Tb}^{3+}$  chelate fluorescent nanoparticle-labeled SA (A) and the BPTA- $\text{Tb}^{3+}$  chelate-labeled SA (B) for human PSA.

SA can be directly used for the bioassay. Unexpectedly, the TR-FIA of human PSA using this nanoparticle-labeled SA gave very large CV ( $\sim 8\text{--}12\%$ ) for fluorescence measurement. This may be caused by the existence of trace agglomerated nanoparticles (produced in the surface modification and labeling procedures) in the labeled SA solution. After the nanoparticle-labeled SA was purified by Sephadex G-50 filtration chromatography (Figure 5), a uniform solution of the nanoparticle-labeled SA was obtained. The TR-FIA using the purified nanoparticle-labeled SA gave good measurement precision (the signal CVs are in the range of 1.5–5.5% and the concentration CVs in the range of 4–14%).

**Time-Resolved Fluoroimmunoassay of Human PSA.** The PSA in human serum as a important tumor marker has been widely accepted and used in the diagnosis of prostatic cancer<sup>34,35</sup> and breast cancer<sup>35</sup> and has been measured with various immunoassays, i.e., enzyme immunoassay,<sup>36</sup> radioimmunoassay,<sup>37</sup> chemiluminescence immunoassay,<sup>38</sup> and TR-FIA.<sup>39,40</sup> Yu et al. reported

(30) Sueda, S.; Yuan, J.; Matsumoto, K. *Bioconjugate Chem.* **2002**, *13*, 200–205.

(31) Hermanson, G. T.; Mallia, A. K.; Smith, P. K. *Immobilized Affinity Ligand Techniques*; Academic Press Inc.: New York, 1992.

(32) Schena, M.; Shalon, D.; Heller, R.; Chai, A.; Brown, P. O.; Davis, R. W. *Proc. Natl. Acad. Sci. U.S.A.* **1996**, *93*, 10614–10619.

(33) Yuan, J.; Wang, G.; Kimura, H.; Matsumoto, K. *Anal. Biochem.* **1997**, *254*, 283–287.

(34) Armbruster, D. A. *Clin. Chem.* **1993**, *39*, 181–195.

(35) Ferguson, R. A.; Yu, H.; Kalyvas, M.; Zammit, S.; Diamandis, E. P. *Clin. Chem.* **1996**, *42*, 675–684.

(36) Vessella, R. L.; Noteboom, J.; Lange, P. H. *Clin. Chem.* **1992**, *38*, 2044–2054.

(37) Doi, D. S.; Pronovost, C.; Escares, E. *Clin. Chem.* **1990**, *36*, 1050.

(38) Dudley, R. F. *Lab. Med.* **1990**, *21*, 216–222.

that prostate cancer relapse could be diagnosed over one year earlier with a sensitive PSA assay having a detection limit of 20 pg/mL than with assays having detection limits of 100 pg/mL or higher.<sup>39</sup> Therefore, the immunoassay of PSA was used to evaluate the usefulness of the Tb<sup>3+</sup> chelate nanoparticle-labeled SA for TR-FIA.

The calibration curve of TR-FIA for PSA using the silica-coated Tb<sup>3+</sup> chelate nanoparticle-labeled SA is shown in Figure 6A. The straight line in the PSA concentration range of 0.001–1 ng/mL can be expressed as  $\log(\text{signal}) = 0.377 \log[\text{PSA}] + 3.66$  ( $r = 0.998$ ). The smaller slope of the calibration curve might be caused by the different efficiency of the labeled SA-biotinylated antibody reaction on the solid-phase surface at different antigen concentration. It is possible that the more dense the antigen is on the solid-phase surface, the more difficult it is to detect the biotinylated antibodies on the surface using the nanoparticle-labeled SA with an equal efficiency due to the effect of the steric hindrance among the nanoparticles on the solid-phase surface. The detection limit, defined as the concentration corresponding to 3 standard deviations of background signal, is 7.0 pg/mL. The calibration curve of PSA using the BPTA–Tb<sup>3+</sup> chelate-labeled SA instead of the nanoparticle-labeled SA is shown in Figure 6B. This method gives a detection limit of 59 pg/mL. The comparison of the detection limits of the two methods shows that the sensitivity of TR-FIA is improved ~8 times by using the nanoparticle-labeled SA instead of the BPTA–Tb<sup>3+</sup> chelate-labeled SA. This result indicates that the use of silica-coated lanthanide chelate fluorescent nanoparticles as the probe for TR-FIA is more favorable than the use of lanthanide chelate.

(39) Yu, H.; Diamandis, E. P.; Prestigiacomo, A. F.; Stamey, T. A. *Clin. Chem.* **1995**, *41*, 430–434.

(40) Qin, Q.-P.; Lövgren, T.; Pettersson, K. *Anal. Chem.* **2001**, *73*, 1521–1529.

## CONCLUSION

In the present work, preparation, characterization, and time-resolved fluorometric application of the strongly fluorescent silica-coated Tb<sup>3+</sup> chelate nanoparticles that have uniform size and high photostability are reported for the first time. The nanoparticle's surface was modified and covalently coupled to SA successfully by a new stable method. The new method would be also very useful for efficient preparation of nanoparticle conjugates with biomolecules, such as antibody, antigen, enzyme, and nucleic acid. The TR-FIA application of the nanoparticle-labeled SA shows that the nanoparticles are favorably useful as a new type fluorescence probe for time-resolved fluorometry. Although the results are primary, the properties of strong fluorescence, long fluorescence lifetime, and good photostability of the nanoparticles suggest that the new type fluorescent nanoparticles are also very attractive for highly sensitive time-resolved fluorescence cyto- and histochemistry imaging technologies. As the labeling and time-resolved fluorometric technologies improved in recent years, the new fluorescence reagent can also be expected to promote the application of highly sensitive detection technology in biological analysis.

## ACKNOWLEDGMENT

This work was supported by the National Natural Science Foundation of China (20175027).

Received for review May 2, 2003. Accepted September 11, 2003.

AC030177M